tapraid4/z4g-trj/z4g-trj/z4g00905/z4g1442d05g | tillotsj | S=18 | 8/19/05 | 20:57 | Art: 057957



# Nonlinear Buckling of Woven Fabrics. Part I: Elastic and Nonelastic Cases

R. D. ANANDJIWALA[1]

*National Fibre, Textile and Clothing Centre, CSIR Manufacturing & Materials Technology, and Department of Textile Science, Nelson Mandela Metropolitan University, Port Elizabeth, South Africa.*

J. W. GONSALVES

*Department of Mathematics and Applied Mathematics, Nelson Mandela Metropolitan University, Port Elizabeth 6000, South Africa.*

ABSTRACT

The fabric buckling model proposed by Grosberg and Swani has been modified by incorporating Huang's bilinear bending rule. The proposed model is an extension of the present model and also covers the special cases. The numerical results appear realistic and conform to the trend observed by other researchers. The effects of fabric bending parameters on the buckling behavior of woven fabrics were explored by numerical computations. The second part of this paper includes the recovery from large-scale buckling of woven fabric.

Fn1

The buckling, bending and drape behaviors of a woven fabric influence its performance during actual use and during the process of making-up into the end product. These properties are important, particularly when the fabric is limp, resulting in large-scale deformation even under small applied forces. The buckling properties of a woven fabric also influence the sewing of garments and their resultant quality. Moreover, the development of robotized sewing operations for reducing unit production cost is critically important if garment industries in developed countries are keen to improve their competitiveness *vis-à-vis* low labor cost countries [4, 5]. This has placed a great responsibility on textile engineers to develop appropriate mathematical models which are capable of providing realistic information with minimum complexities, mathematical drudgery and computational cost. Of course, these models should be based on logical assumptions reflecting the real physical phenomena, yet simple to solve for simulating real fabric behavior.

The complexity of textile mechanics in solving the above problems is complicated by the fact that this discipline of textile science, despite considerable research efforts, is based on divergent approaches rather than on sound fundamental concepts developed after debate and criticism and validated by competent researchers for universal acceptance [10]. The mechanics of the buckling behavior of woven fabric is not an exception to this as seen from the large number of different approaches found when scanning the literature. It started with the classical paper by Grosberg and Swani [7] who built a simple buckling model based on Grosberg's idealized bending rule [6], taking into account the frictional effect and following the principles of elastic buckling theory for struts reported in classical mechanics [13, 14]. Their model assumed an *infinitely* large bending rigidity of the cloth for the initial nonlinear region of the bending curve where the applied couple had not yet overcome the frictional restraining couple. They noted, however, that, in practice, real fabrics are fairly rigid for the initial bending region, but they are not infinitely rigid as assumed in the idealized bending rule [6]. Nevertheless, they continued to build their buckling model on the basis of the idealized bending rule in order to avoid the complications arising from the additional mathematical treatments required to obtain the precise solutions. Clap and Peng [4, 5] later developed a model by utilizing Timoshenko's elastica theory [14] in which they assumed the fabric as a curved beam of constant cross-section. They introduced the effect of fabric weight, which was ignored by Grosberg and Swani [7], but again followed the same frictional restraining principle of infinite initial bending rigidity as proposed by Grosberg [6]. More recently, Kang *et al.* [9] used regression analysis to fit an exponential function to initial nonlinear fabric bending behavior and utilized the derived relationship in building a buckling model similar to that proposed by Clap and Peng [4, 5] based on the assumption

[1] To whom correspondence should be addressed: e-mail: rajesh.anandjiwala@nmmu.ac.za

 

tapraid4/z4g-trj/z4g-trj/z4g00905/z4g1442d05g | tillotsj | S=18 | 8/19/05 | 20:57 | Art: 057957



that the fabric is a continuum of a thin solid beam. The governing equations of Timoshenko's elastica theory [14] and the Bernoulli–Euler's theorem from classical mechanics could therefore be directly employed. It may be argued, however, based on detailed analyses of various authors, that the bending behavior of a real fabric is markedly different from that of a symmetrical solid beam [1, 6, 12]. Unlike the classical beam theory in solid mechanics, the bending curves of real fabric above and below the neutral axis do not exhibit the same magnitude of extension and contraction. In fact, the fabric experiences a progressively increasing extension above the neutral axis and progressively increasing compression below the neutral axis.

Huang [8] modified Grosberg's [6] idealized bending rule by incorporating bilinearity, which was further utilized by Leaf and Anandjiwala [11] in proposing a generalized model of a plain woven fabric and subsequently for modifying Huang's extension analysis [3]. Although, Kang *et al.* [9] have utilized Huang's bilinearity in their model, the obvious inconsistency of applying the classical beam theory to the textile problem remains. Frictional restraint to bending of the fabric arises from inter-fiber frictional forces resulting from the fact that the fibers act as individual units and do not form a solid beam. Nevertheless, it is interesting to note that Kang *et al.* [9] themselves have observed better results when incorporating Huang's bilinear bending behavior [8] into their model than when using their own exponential function! This reaffirms our belief in the bilinear bending rule [8], which is a more reasonable and realistic approximation of the real bending behavior of yarn and fabrics, but relatively easy to handle in mathematical analysis in comparison with the exponential nonlinearity proposed by Kang *et al.* [9] and the quadratic nonlinearity by Abbott *et al.* [1].

In this paper we have modified Grosberg and Swani's buckling theory [7] for woven fabric by introducing Huang's bilinear bending rule [8]. The assumption of infinitely high initial bending rigidity of the fabric in their model [7] is thus removed. The proposed theory also eliminates obvious inconsistencies in several earlier approaches [4–7, 13] based on Grosberg's idealized bending rule. The methodology of the theoretical treatment employed here is similar to that proposed in an earlier paper by Leaf and Anandjiwala [11] but is further suitably modified to accommodate both Grosberg and Swani's model [7] and elastic buckling theory of classical engineering mechanics [13, 14] as special cases. A numerical solution of the model is developed and numerical results are presented to study the effect of fabric bending parameters, such as initial and final bending rigidities, $B^*$ and $B$, respectively, and transition couple, $M_a$ on the buckling of woven fabric.

## Theoretical

Consider a piece of fabric, of length $l$, buckled under a vertical point force $P$ to create a large-scale deflection as shown in Figure 1, with the one end of the fabric fixed at the origin O of the Cartesian co-ordinates. The compressed height $Y$ of the fabric under the force $P$ along the $Y$-axis is given by $Y = 2y_A + y_2$ as shown in the figure. Let OZ be the half length of the fabric and the deflection of the fabric at Z along the $X$-axis be denoted by $D$. It is assumed that the fabric obeys Huang's bilinear bending rule as given below [8]:

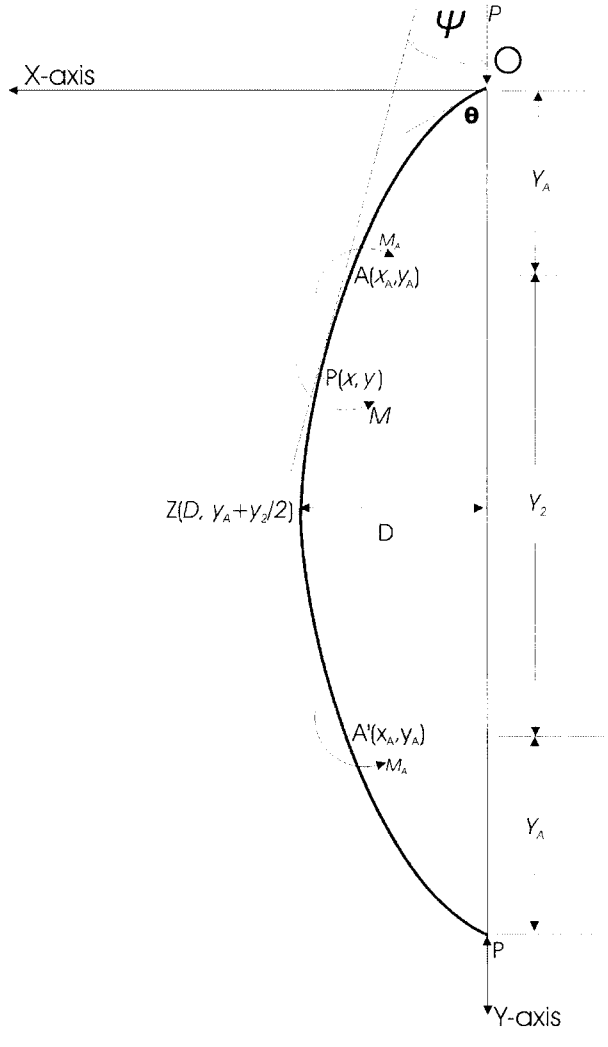


FIGURE 1. Force–compression curve of a buckled fabric.

$$K = \frac{M}{B^*} \qquad M \le M_a \tag{1}$$

$$K = \frac{M_a}{B^*} + \frac{M - M_a}{B} \qquad M > M_a \tag{2}$$

where $K$ is the curvature, $M$ is the moment, $M_a$ is the transition couple and $B^*$ and $B$ are the initial and final bending rigidities, respectively. The point A $(x_A,y_A)$ in Figure 1 is a boundary point at which the applied moment $M$ begins to overcome the transition couple which is related to the frictional couple, $M_o$, proposed by Grosberg [6] by the following relationship:

$$M_a = \frac{M_o}{\left(1 - \frac{B}{B^*}\right)} \tag{3}$$

Consider now any general point P $(x,y)$ on the bending curve which lies between the origin, O and the mid-point of the fabric denoted by Z. The angle subtended by the tangent to any point P $(x,y)$ with respect to $Y$-axis is denoted by $\psi$ and the angle at the origin, which is a point of inflexion, is denoted by $\theta$.

Next consider a general point P $(x,y)$ on OA such that it follows the bending rule given in equation (1) and the arc length OP is given by $s$. At the boundary point A, $s = l_1$, $x = x_A$ and $y = y_A$. Following the methodology proposed in a previous paper by Leaf and Anandjiwala [11] the governing equations for the section OA are as follows:

$$l_1 = \sqrt{\frac{B^*}{P}}\left\{F\left(k^*,\frac{\pi}{2}\right) - F(k^*,\phi_A^*)\right\} \tag{4}$$

$$x_A = 2k^*\sqrt{\frac{B^*}{P}}\cos\phi_A^* \tag{5}$$

$$y_A = \sqrt{\frac{B^*}{P}}\left[2\left\{E\left(k^*,\frac{\pi}{2}\right) - E(k^*,\phi_A^*)\right\} - \left\{F\left(k^*,\frac{\pi}{2}\right) - F(k^*,\phi_A^*)\right\}\right] \tag{6}$$

where

$$k^* = \sin\frac{\theta}{2} \tag{7}$$

$$\psi_A = \cos^{-1}\left(\cos\theta + \frac{M_a^2}{2PB^*}\right) \tag{8}$$

$$\phi_A^* = \sin^{-1}\left(\frac{\sin\frac{\psi_A}{2}}{k^*}\right) \tag{9}$$

$F\left(k^*,\frac{\pi}{2}\right)$ *and* $F(k^*,\phi_A^*)$ are complete and incomplete elliptic integrals of the first kind, and $E\left(k^*,\frac{\pi}{2}\right)$ *and* $E(k^*,\phi_A^*)$ are complete and incomplete elliptic integrals of the second kind.

Consider now a general point P $(x,y)$ on AZ such that it follows the bending rule given in equation (2) and the arc length OP is given by $s$. At the boundary point Z, $\psi = 0$, $s = l/2 = (l_1 + 0.5l_2)$, $x = D$ and $y = (y_A + 0.5y_2)$. Following the methodology proposed in a previous paper by Leaf and Anandjiwala [11] the governing equations for the section AZ are as follows:

$$\frac{1}{2} = \sqrt{\frac{B}{P}}\{F(k,\phi_A)\} + l_1 \tag{10}$$

$$D = 2k\sqrt{\frac{B}{P}}(1 - \cos\phi_A) + x_A \tag{11}$$

$$\frac{y_2}{2} = \sqrt{\frac{B}{P}}\{2E(k,\phi_A) - F(k,\phi_A)\} \tag{12}$$

where,

$$k = \sqrt{k^{*2} - \frac{M_a^2}{4PB^*}\left(1 - \frac{B}{B^*}\right)} \tag{13}$$

$$\phi_A = \sin^{-1}\left(\frac{k^*\sin\phi_A^*}{k}\right) \tag{14}$$

$$\psi_2 = 0 \tag{15}$$

The fractional compression $\delta$ is then given by:

$$\delta = 1 - \frac{2y_A + y_2}{2l_1 + l_2} \tag{16}$$

$F(k,\phi_A)$ *and* $E(k,\phi_A)$ $F(k,\phi_A)$ and $E(k,\phi_A)$ are the incomplete elliptic integrals of the first and the second kind, respectively. AQ: 3

## GROSBERG'S BUCKLING MODEL

Grosberg and Swani [7] assumed a bending law [6] in which the initial bending rigidity $B^*$ tends to infinity and therefore the initial region OA was assumed to be a straight line with curvature $K = 0$, which implies that $(B/B^*) = 0$, therefore, from equation (3) $M_a = M_o$. By substituting this in equations (4) to (15) and deriving the simple trigonometric relationships for the initial straight line region OA, the following is obtained:

$$\frac{l}{2} = \sqrt{\frac{B}{P}}\left\{F\left(k,\frac{\pi}{2}\right)\right\} + \frac{M_o}{P}\operatorname{cosec}\theta \tag{18}$$

tapraid4/z4g-trj/z4g-trj/z4g00905/z4g1442d05g | tillotsj | S=18 | 8/19/05 | 20:57 | Art: 057957



$$D = 2k\sqrt{\frac{B}{P}} + \frac{M_0}{P} \tag{19}$$

$$\frac{y_2}{2} = \sqrt{\frac{B}{P}}\left\{2E\left(k,\frac{\pi}{2}\right) - F\left(k,\frac{\pi}{2}\right)\right\} \tag{20}$$

$$y_A = \frac{M_0}{P}\cot\theta \tag{21}$$

Equations (18) to (21) are identical to the buckling model reported by Grosberg and Swani [7].

### Elastic Buckling Model

The elastic buckling theory in classical mechanics assumed a linear relationship between moment and curvature, ignoring the effect of the frictional couple which influences the behavior of textile materials, such as yarns and fabrics. This implies that $M_a = 0$ and $B = B^*$. When substituting these values in equations (4) to (16) equations are obtained that are similar to the buckling of a strut reported in standard textbooks of mechanics [13, 14].

## Numerical Results and Discussion

The governing equations for solving the model proposed above were converted into non-dimensional forms by using $B/l^2$ as unit force and $l$ as unit length. Then the governing equations in non-dimensional forms were solved for a known non-dimensional force, $\bar{P} = \frac{Pl^2}{B}$, fabric bending parameters, such as, $\overline{M_a} = \frac{M_a l}{B}$ and $\lambda^2 = \frac{B}{B^*}$ and by estimating the value of $\theta$ which is unknown. The computation was continued until the initial estimate of $\theta$ is modified to satisfy the known boundary conditions, namely, $l = 0.5$ and $\psi_Z = 0$ within specified tolerance limits. From the calculated values of the parameters, the fractional compression, $\delta$, was calculated for a known non-dimensionless force $\frac{Pl^2}{B}$. Thus, by systematically varying the values of $\frac{Pl^2}{B}$ in a realistic range, a theoretical buckling curve for a woven fabric can be plotted for the known fabric bending parameters. The values of $\overline{M_a} = \frac{M_a l}{B}$, $\lambda^2 = \frac{B}{B^*}$, $B$ and $B^*$ were systematically varied within a range to study the effect of fabric bending parameters on the buckling of the woven fabrics. The corresponding buckling curves for two special cases discussed above were also calculated.

### Effect of $\overline{M_a}$ and $\lambda^2$

Figure 2 shows the theoretical buckling curves of woven fabrics for different values of $\lambda^2$ at a constant value of $\overline{M_a} = \frac{M_a l}{B}$. The value of $\overline{M_a}$ is also changed systematically as shown in Figure 2a to d. For each value of $\overline{M_a}$, the values for $\lambda^2$ are systematically varied from 0, for Grosberg's case, to 0.2, 0.5 and 0.8 for the bilinear buckling model. Furthermore, the elastic buckling case is plotted for $\overline{M_a} = 0$ and $\lambda^2 = 1.0$ for comparison with the

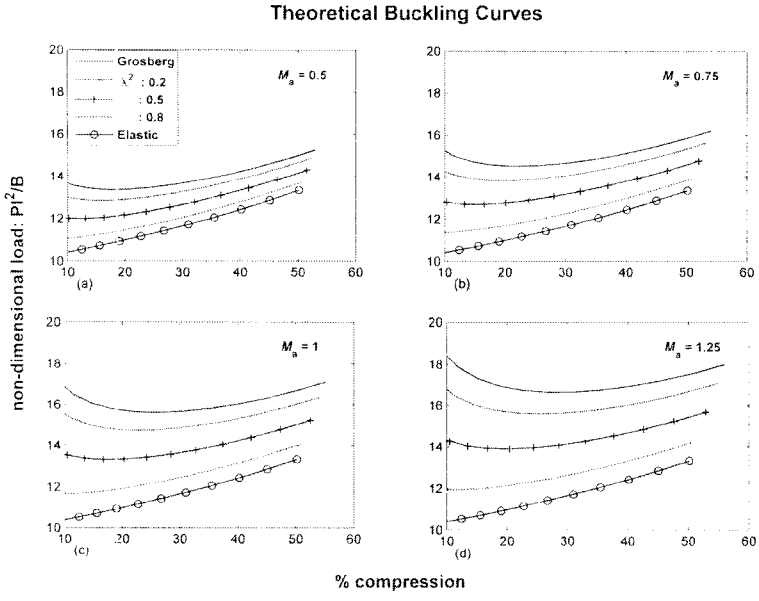


FIGURE 2. Effect of $\lambda^2$ on fabric buckling for (a) $\overline{M_a} = 0.5$, (b) $\overline{M_a} = 0.75$, (c) $\overline{M_a} = 1.0$ and (d) $\overline{M_a} = 1.25$.

tapraid4/z4g-trj/z4g-trj/z4g00905/z4g1442d05g | tillotsj | S=18 | 8/19/05 | 20:57 | Art: 057957



TABLE 1. Calculated values of the non-dimensionless force, $\frac{Pl^2}{B}$, at various values of percentage compression, $\overline{M_a} = \frac{M_a l}{B}$ and $\lambda^2$.

| | $\overline{M_a} = 0.5$ | | | $\overline{M_a} = 0.75$ | | | $\overline{M_a} = 1.0$ | | | $\overline{M_a} = 1.25$ | | |
|---|---|---|---|---|---|---|---|---|---|---|---|---|
| % compression | 10 | 30 | 50 | 10 | 30 | 50 | 10 | 30 | 50 | 10 | 30 | 50 |
| Grosberg | 13.66 | 13.67 | 15.01 | 15.27 | 14.67 | 15.85 | 16.85 | 15.66 | 16.68 | 18.41 | 16.65 | 17.51 |
| $\lambda^2 = 0.3$ | 13.00 | 13.27 | 14.68 | 14.28 | 14.07 | 15.35 | 15.54 | 14.86 | 16.01 | 16.78 | 15.64 | 16.67 |
| $\lambda^2 = 0.5$ | 12.02 | 12.66 | 14.17 | 12.81 | 13.16 | 14.59 | 13.58 | 13.66 | 15.01 | 14.34 | 14.15 | 15.42 |
| $\lambda^2 = 0.8$ | 11.04 | 12.06 | 13.66 | 11.35 | 12.26 | 13.83 | 11.65 | 12.46 | 13.99 | 11.94 | 12.65 | 14.16 |
| Elastica | 10.39 | 11.65 | 13.32 | 10.39 | 11.65 | 13.32 | 10.39 | 11.65 | 13.32 | 10.39 | 11.65 | 13.32 |

theoretical curves. The numerical results obtained from the present model are consistent with results reported by other researchers [4, 5, 7, 9]. As expected, at constant value of $\overline{M_a}$, in general, the load required to buckle the fabric at the same percentage compression level increases as the value of $\lambda^2$ decreases from 1 for elastic buckling to 0 for Grosberg's case, other values of $\lambda^2$ taking intermediate values in decreasing order, for the bilinear buckling model. The corresponding values of the calculated non-dimensional force $\frac{Pl^2}{B}$, at various values of $\overline{M_a}$, percentage compression and $\lambda^2$ are given in Table 1 for better clarity of the observed trends. As can be seen from Table 1, the values of the non-dimensional force increases from 11.65 for elastic buckling to 13.67 for Grosberg's model for $\overline{M_a} = 0.5$ and percentage contraction = 30; the bilinear model giving intermediate values of 12.06, 12.66, and 13.27 for $\lambda^2$ values of 0.8, 0.5 and 0.3, respectively. The trend observed is consistent in all cases as can be seen from Table 1. This is due to the fact that the bending resistance of the fabric in elastic buckling is minimal and progressively increases as the value of $\lambda^2$ decreases, with the maximum bending resistance at $\lambda^2 = 0$ for the Grosberg's model, where the initial bending region is assumed to be infinitely rigid. This implies that the elastic buckling case underestimates the required buckling load, whereas Grosberg's model overestimates it. The present model, based on the bilinear bending rule, therefore, provides the correction to these two extreme theoretical cases, which is based on the experimentally measurable bending parameters.

Figure 3 shows the theoretical buckling curves of woven fabrics for different values of $\overline{M_a}$ but at a constant value of $\lambda^2$. To reconfirm the trend observed in the previous paragraphs, different values of $\overline{M_a}$ and $\lambda^2$ are chosen in this computation in comparison to Figure 2. The values of $\lambda^2$ are also varied as shown in Figures 3a to d. From these figures, in general, as the value of $\overline{M_a}$ increases at a constant value of $\lambda^2$, the load required to buckle the fabric at a constant percentage compression level also increases. The increase in $\overline{M_a}$ at a constant $\lambda^2$ (ratio of $B$ to $B^*$) implies the requirement of a higher frictional couple which opposes the initial bending of the

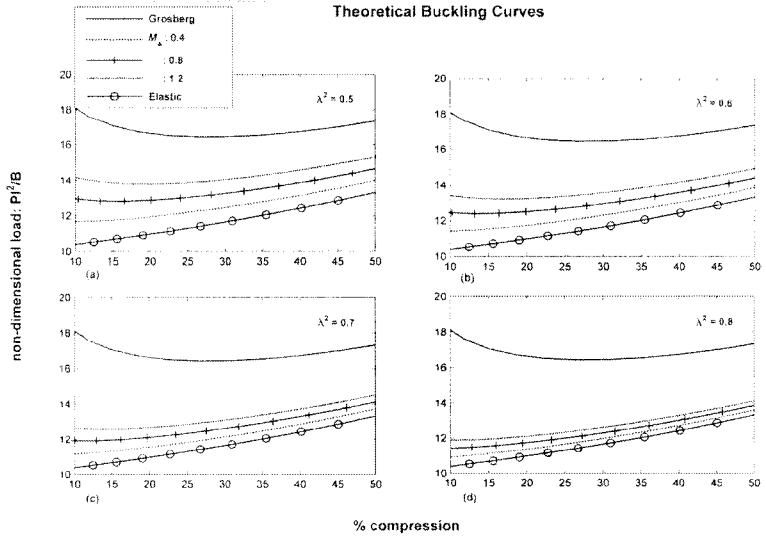


FIGURE 3. Effect of $\overline{M_a}$ on fabric buckling for (a) $\lambda^2 = 0.5$, (b) $\lambda^2 = 0.6$, (c) $\lambda^2 = 0.7$ and (d) $\lambda^2 = 0.8$.

tapraid4/z4g-trj/z4g-trj/z4g00905/z4g1442d05g | tillotsj | S=18 | 8/19/05 | 20:57 | Art: 057957



fabric due to the restriction of yarn slippage at interlacings and also due to inter-fiber frictional resistance which prevents easy bending of the fibers in the yarns, leading to increased resistance to buckling. Table I also shows the calculated values of the non-dimensional force for different values of $\overline{M_a}$ at constant values of percentage compression and $\lambda^2$. At $\lambda^2 = 0.5$ and percentage compression = 30, the calculated values of the non-dimensional force are 12.66, 13.16, 13.66 and 14.15 for corresponding values of 0.5, 0.75, 1.0 and 1.25 for $\overline{M_a}$, respectively. The increase in $\overline{M_a}$ at a constant $\lambda^2$ (ratio of $B$ to $B^*$) also implies increased hysteresis in bending. The effect of hysteresis in bending on buckling and recovery will be discussed in detail in the second part of this paper. The results obtained here are consistent with the published reports by other researchers [4, 5, 7, 9]. To compare the bilinear buckling model with the elastic buckling and Grosberg's models, they have also been plotted on the same graph as shown in Figure 3. As expected, these two special cases of the present model occupy two extreme positions. Once again, the elastic buckling model underestimates the required buckling load whereas that of Grosberg's model overestimates it. The present model, therefore, provides the necessary correction to these two extreme theoretical cases, which is based on the experimentally measurable bending parameters.

## EFFECTS OF INITIAL ($B^*$) AND FINAL ($B$) BENDING RIGIDITIES

F4 Figure 4 shows the theoretical buckling curves of woven fabrics for different values of $B^*$ at constant values of $\overline{M_a}$ and final bending rigidity, $B$. The values of $\overline{M_a}$ are also changed systematically as shown in Figure 4a to d. For each value of $\overline{M_a}$ and $B$, the values of $B^*$ are systematically varied from 5 to 15 in steps of 5, the Grosberg's and the elastic buckling graphs also being shown for comparison. The non-dimensional load, $\frac{Pl^2}{B}$, at constant values of percentage compression, $\overline{M_a}$ and $B$, increases with an increase in initial bending rigidity as shown in Figure 4a. The increase in initial bending rigidity, $B^*$, implies that the initial resistance to buckling increases. In general, the lowest buckling load is required for elastic buckling and the highest for Grosberg's model where the value of $B^*$ tends to infinity, while all bilinear cases occupy intermediate positions between these two extreme cases as shown in Figure 4a to d. The increase in initial bending rigidity, $B^*$, at constant $\overline{M_a}$ and final bending rigidity, $B$; implies that the fabric will require a higher load for the onset of buckling. This resistance results from the frictional forces restricting the movement of the yarns and fibers. This frictional force is produced by a pressure which arises from inter-yarn forces at intersections due to yarn interlacings in the woven fabric. The real effect of this frictional force is to produce the coercive couple which has to be overcome before any bending takes place [6]. Table 2 shows the T2 calculated values of the non-dimensional force, $\frac{Pl^2}{B}$, for a constant value of the final bending rigidity, $B$, but with different values for percentage compression, $\overline{M_a}$, and initial bending rigidity, $B^*$. For $\overline{M_a} = 0.5$ and 30%

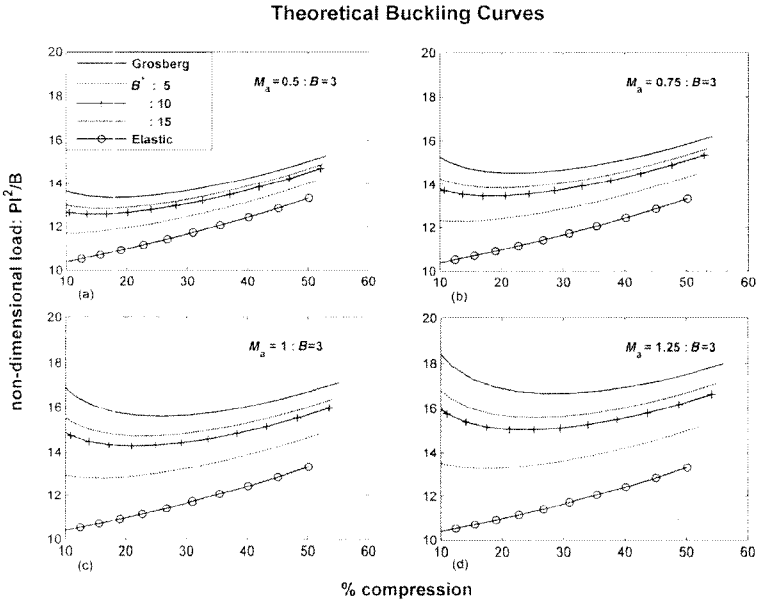


FIGURE 4. Effect of the initial bending rigidity, $B^*$ at a constant value of the final bending rigidity, $B$, for (a) $\overline{M_a} = 0.5$, (b) $\overline{M_a} = 0.75$, (c) $\overline{M_a} = 1.0$ and (d) $\overline{M_a} = 1.25$.

TABLE 2. Calculated values of the non-dimensionless force, $\frac{Pl^2}{B}$, at various values of percentage compression, $\overline{M_a} = \frac{M_a l}{B}$ and $B^*$, $B = 3$ = constant.

| | $\overline{M_a}$ = 0.5 | | | $\overline{M_a}$ = 0.75 | | | $\overline{M_a}$ = 1.0 | | | $\overline{M_a}$ = 1.25 | | |
|---|---|---|---|---|---|---|---|---|---|---|---|---|
| % compression | 10 | 30 | 50 | 10 | 30 | 50 | 10 | 30 | 50 | 10 | 30 | 50 |
| Elastica | 10.39 | 11.65 | 13.32 | 10.39 | 11.65 | 13.32 | 10.39 | 11.65 | 13.32 | 10.39 | 11.65 | 13.32 |
| $B^*$ = 5 | 11.69 | 12.46 | 14.00 | 12.32 | 12.86 | 14.34 | 12.94 | 13.26 | 14.67 | 13.53 | 13.65 | 15.00 |
| $B^*$ = 10 | 12.67 | 13.07 | 14.51 | 13.79 | 13.33 | 15.09 | 14.89 | 14.46 | 15.68 | 15.97 | 15.14 | 16.25 |
| $B^*$ = 15 | 13.00 | 13.27 | 14.68 | 14.28 | 14.07 | 15.36 | 15.54 | 14.86 | 16.01 | 16.79 | 15.64 | 16.67 |
| Grosberg | 13.66 | 13.67 | 15.01 | 15.27 | 14.67 | 15.85 | 16.85 | 15.66 | 16.68 | 18.41 | 16.65 | 17.51 |

compression, the values of the non-dimensional force increases from 11.65 for elastic buckling to 12.46, 13.07 and 13.27 for $B^*$ values of 5, 10 and 15, respectively, with the highest value of 13.67 for Grosberg's model where $B^*$ tends to infinity. As observed in the previous section, the calculated values of the non-dimensional buckling load required to produce the same percentage compression increases with an increase in $\overline{M_a}$. For example, as shown in Table 2, at $B^*$ = 10, and percentage compression = 30, the corresponding non-dimensional loads are 13.07, 13.33, 14.46 and 15.14 for $\overline{M_a}$ values of 0.5, 0.75, 1.0 and 1.25, respectively.

F5 Figure 5 shows the theoretical buckling curves of woven fabrics for different values of $B$ and at constant values of $\overline{M_a}$ and initial bending rigidity, $B^*$. The values of $\overline{M_a}$ are also varied systematically as shown in Figure 5a to d. For each value of $\overline{M_a}$ and $B^*$, the values of $B$ are systematically varied from 5, to 10 in steps of 2.5, together with the Grosberg and elastic buckling cases calculated for comparison purposes. The non-dimensional load, $\frac{Pl^2}{B}$, at constant values of percentage compression, $\overline{M_a}$ and $B^*$, decreases with an increase in final bending rigidity as shown in Figure 5a. The increase in final bending rigidity, $B$, at a constant value of initial bending rigidity, $B^*$, implies that the buckling of the fabric becomes relatively easy since the initial resistance arising from frictional restraint mechanism is already overcome. Moreover, $\lambda^2$ is the ratio of $B$ to $B^*$, which tends to unity signifying that the buckling of the fabric becomes close to elastic buckling. The reduction in the values of the final bending rigidity at a constant value of $B^*$ implies that the ratio $\lambda^2$ tends to zero which signifies that the fabric resists buckling, similar to Grosberg's model. Table 3 shows the calculated values of the non- T3

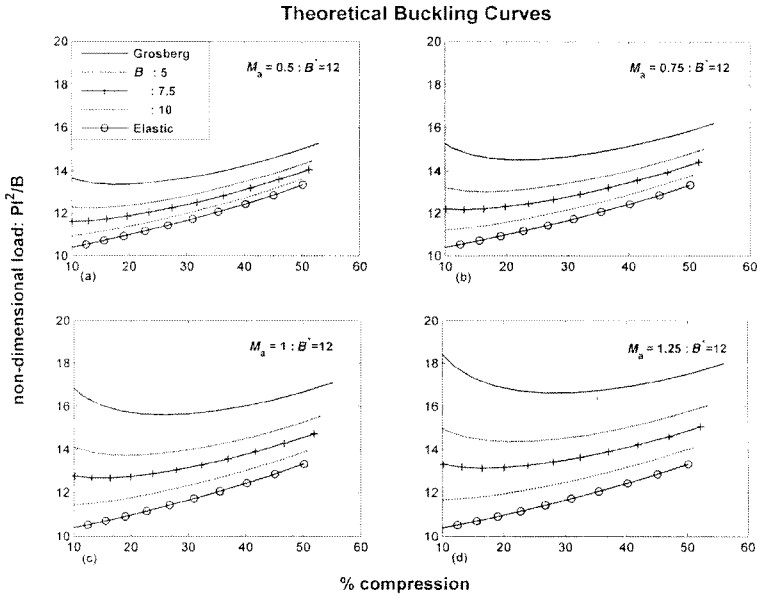


FIGURE 5. Effect of the final bending rigidity, $B$ at a constant value of the initial bending rigidity, $B^*$, for (a) $\overline{M_a}$ = 0.5, (b) $\overline{M_a}$ = 0.75, (c) $\overline{M_a}$ = 1.0 and (d) $\overline{M_a}$ = 1.25.

tapraid4/z4g-trj/z4g-trj/z4g00905/z4g1442d05g | tillotsj | S=18 | 8/19/05 | 20:57 | Art: 057957



TABLE 3. Calculated values of the non-dimensionless force, $\frac{Pl^2}{B}$, at various values of percentage compression, $\overline{M_a}=\frac{M_a l}{B}$ and $B$, $B^* = 12$ = constant.

| | $\overline{M_a}$ = 0.5 | | | $\overline{M_a}$ = 0.75 | | | $\overline{M_a}$ = 1.0 | | | $\overline{M_a}$ = 1.25 | | |
|---|---|---|---|---|---|---|---|---|---|---|---|---|
| % compression | 10 | 30 | 50 | 10 | 30 | 50 | 10 | 30 | 50 | 10 | 30 | 50 |
| Grosberg | 13.66 | 13.67 | 15.01 | 15.27 | 14.67 | 15.85 | 16.85 | 15.66 | 16.68 | 18.41 | 16.65 | 17.51 |
| $B$ = 5 | 12.29 | 12.83 | 14.31 | 13.22 | 13.41 | 14.80 | 14.13 | 13.99 | 15.29 | 15.02 | 14.56 | 15.77 |
| $B$ = 7.5 | 11.61 | 12.41 | 13.96 | 12.20 | 12.79 | 14.27 | 12.78 | 13.16 | 14.59 | 13.33 | 13.52 | 14.90 |
| $B$ = 10 | 10.93 | 11.99 | 13.60 | 11.19 | 12.16 | 13.74 | 11.44 | 12.32 | 13.88 | 11.68 | 12.48 | 14.02 |
| Elastica | 10.39 | 11.65 | 13.32 | 10.39 | 11.65 | 13.32 | 10.39 | 11.65 | 13.32 | 10.39 | 11.65 | 13.32 |

dimensional force, $\frac{Pl^2}{B}$, for a constant value of the final bending rigidity, $B^*$, but with different values of percentage compression, $\overline{M_a}$, and initial bending rigidity, $B$. The calculated values of the non-dimensional buckling load required to produce the same percentage compression increases with an increase in $\overline{M_a}$. For example, as shown in Table 2, at $B$ = 7.5, and percentage compression = 30, the corresponding non-dimensional loads are 12.41, 12.79, 13.16 and 13.52 for $\overline{M_a}$ values of 0.5, 0.75, 1.0 and 1.25, respectively.

The foregoing discussions based on numerical results indicate that the buckling behavior of a fabric based on bilinear bending rule can be calculated from experimentally measurable bending parameters, such as the frictional couple, and the initial and final bending rigidities. An extensive numerical analysis has been undertaken to verify the theoretical behavior of the proposed model within a realistic range of input parameters. Based on the numerical work, graphical nomograms and corresponding tables have been prepared which can help to know the buckling behavior. It is felt that these nomograms and tables will be very useful information for estimating the buckling behavior of a fabric without having to go through the computational exercise that was done in this work. All relevant nomograms and corresponding tables have been stored in the electronic format and can be made available to interested readers upon request to authors.

## Conclusions

The theoretical buckling model of fabric presented here, which is based on the bilinear bending rule, modifies Grosberg and Swani's buckling model. The proposed model also includes, as subsets, other models, such as that of Grosberg and Swani and the elastic buckling models. The proposed model behaves well numerically and its solution can be easily obtained by utilizing established and commercially available numerical analyses programs. The numerical results appear realistic and are consistent with theoretical assumptions. The second part of this paper will deal with the recovery behavior of the fabric buckled to a finite deformation, the effect of bending hysteresis, and experimental validation of the theory.

ACKNOWLEDGEMENT

Dr John Gonsalves acknowledges the Nelson Mandela Metropolitan University for granting him sabbatical research leave to take part in this ongoing research at the National Fibre, Textile & Clothing Centre, Manufacturing and Materials Technology, CSIR, South Africa.

## Appendix

NOMENCLATURE

$l$ = length of fabric
$P$ = vertical point force
$Y$ = compressed height of the fabric
$y_A$ = $Y$-coordinate of point A
$x_A$ = $X$-coordinate of point A
$s$ = length of fabric measured from the origin O to any point P $(x,y)$
$l_1$ = length of fabric from origin O to point A $(x_A,y_A)$
$l_2/2$ = length of fabric from point A to the half length of the fabric at point Z
$y_2/2$ = compressed height of the fabric from point A to the half length of the fabric at point Z
$D$ = deflection of the fabric at point Z along the $X$-axis
$K$ = curvature of the fabric
$M$ = moment at any point P $(x,y)$
$M_a$ = transition couple
$B^*$ = initial bending rigidity of the fabric
$B$ = final bending rigidity of the fabric
$M_o$ = frictional couple
$\psi$ = inclination of tangent to any point P $(x,y)$ with respect to $Y$-axis

tapraid4/z4g-trj/z4g-trj/z4g00905/z4g1442d05g | tillotsj | S=18 | 8/19/05 | 20:57 | Art: 057957



$0$ = $\psi$ at origin O where $s = 0$

$\psi_A$ = inclination of tangent to point A $(x_A, y_A)$ with respect to $Y$-axis

$F\left(k^*, \frac{\pi}{2}\right)$ = complete elliptical integral of the first kind with modulus $k^*$

$E\left(k^*, \frac{\pi}{2}\right)$ = complete elliptical integral of the second kind with modulus $k^*$

$F(k^*, \phi_A^*)$ = incomplete elliptical integral of the first kind with modulus $k^*$ and amplitude $\phi_A^*$

$E(k^*, \phi_A^*)$ = incomplete elliptical integral of the second kind with modulus $k^*$ and amplitude, $\phi_A^*$

$F(k, \phi_A)$ = incomplete elliptical integral of the first kind with modulus $k$ and amplitude $\phi_A$

$E(k, \phi_A)$ = incomplete elliptical integral of the second kind with modulus $k$ and amplitude $\phi_A$

$\delta$ = fractional compression of the fabric

$\psi_Z$ = $\psi$ at point Z

$\bar{P}$ = non-dimensional force = $\frac{Pl^2}{B}$

$\overline{M_a}$ = non-dimensional transitional couple = $\frac{M_a l}{B}$

$\lambda^2$ = ratio of final bending rigidity, $B$ to initial bending rigidity, $B^*$

## Literature Cited


1. Abbott, G. M., Grosberg, P., and Leaf, G. A. V., The Mechanical Properties of Woven Fabrics, Part VII: The Hysteresis During Bending of Woven Fabrics, *Textile Res. J.*, **41,** 345–358 (1971).
2. Amirbayat, J., and Hearle, J. W. S., The Anatomy of Buckling of Textile Fabrics: Drape and Conformability, *J. Text. Inst.*, **80,** 51–68 (1989).
3. Anandjiwala, R. D. and Leaf, G. A. V., Large-Scale Extension and Recovery of Plain Woven Fabrics, Part I: Theoretical, *Textile Res. J.*, **61,** 619–634 (1991).
4. Clap, T. G. and Peng, H., Buckling of Woven Fabrics, Part I: Effect of Fabric Weight, *Textile Res. J.*, **60,** 228–234 (1990).
5. Clap, T. G. and Peng, H., Buckling of Woven Fabrics, Part II: Effect of Weight and Frictional Couple, *Textile Res. J.*, **60,** 285–292 (1990).
6. Grosberg, P., The Mechanical Properties of Woven Fabrics, Part II: The Bending of Woven Fabrics, *Textile Res. J.*, **36,** 205–211 (1966).
7. Grosberg, P. and Swani, N. M., The Mechanical Properties of Woven Fabrics, Part III: The Buckling of Woven Fabrics, *Textile Res. J.*, **36,** 332–338 (1966).
8. Huang, N. C., Finite Biaxial Extension of Completely Set Plain Woven Fabrics, *J. Appl. Mech.*, **46,** 651–655 (1979).
9. Kang, T. J., Joo, K. H., and Lee, K. W., Analyzing Fabric Buckling Based on Nonlinear Bending Properties, *Textile Res. J.*, **74,** 172–177 (2004).
10. Konopasek, M., Afterword, Theoretical Foundations of Textile Science: A Life in and out of Engineering Textiles, *J. Text. Inst.*, **88,** 122–129 (1997).
11. Leaf, G. A. V. and Anandjiwala, R. D., A Generalized Model of Plain Woven Fabric, *Textile Res. J.*, **55,** 92–99 (1985).
12. Livesey, R. G., and Owen, J., Cloth Stiffness and Hysteresis in Bending, *J. Textile Inst.*, **55,** T516–T530 (1964).
13. Southwell, R. V., "An Introduction to the Theory of Elasticity for Engineers and Physicists," Clarendon Press, Oxford, 1936.
14. Timoshenko, S., Strength of Materials, Part I, Van Nostrand Reinhold Co., 1955.


*Manuscript received ?????? ??, 2005; accepted ?????? ?? 2005.*

AQ: 1 AQ: 4

tapraid4/z4g-trj/z4g-trj/z4g00905/z4g1442d05g | tillotsj | S=19 | 8/19/05 | 21:04 | Art: 057957



AQ1—Ref 2 is not cited in text–please add citation or remove from list and renumber all subsequent refs in list and text citations

AQ2— Ed.:x and y to be italic here too?

AQ3— Ed.: dupe copy as meant?

AQ4— Pls. supply received/accepted date.